

General theory and examples of the inverse Frobenius-Perron problem

D. Pingel and P. Schmelcher

*Theoretische Chemie, Physikalisch-Chemisches Institut, Universität Heidelberg,
Im Neuenheimer Feld 253, D-69120 Heidelberg, Germany*

F.K. Diakonos

*Department of Physics, University of Athens, GR-15771 Athens, Greece
(August 13, 2018)*

The general solution of the inverse Frobenius-Perron problem considering the construction of a fully chaotic dynamical system with given invariant density is obtained within the class of one-dimensional unimodal maps. Some interesting connections between this solution and the approach via conjugation transformations are eliminated. The developed method is applied to obtain a wide class of maps having as invariant density the two-parametric beta-probability density function. Varying the parameters of the density a rich variety of dynamics is observed. Observables like autocorrelation functions, power spectra and Lyapunov exponents are calculated for representatives of this family of maps and some theoretical predictions concerning the decay of correlations are tested.

I. INTRODUCTION

One-dimensional iterative maps represent a very useful tool to understand the physics of complex nonlinear systems. In particular they can be used to investigate the different routes of nonlinear dynamical systems from regular to chaotic behaviour [1–3] to simulate physical systems showing anomalous diffusion [4] or to analyse the underlying dynamics in time series with $\frac{1}{f}$ noise in their power spectrum [5,6]. In many cases and in particular from an experimental point of view the only information available for a physical system are its statistical properties (ergodic measure or time correlation function) and one is asked to design a consistent dynamical law. In a recent paper [7] we examined the possibility to construct an one dimensional discrete dynamical system with a given invariant density. This is the so called inverse Frobenius-Perron problem (IFPP) [8–13].

It could be shown that using certain symmetry requirements the IFPP possesses a unique solution. We applied our method to calculate numerically the symmetric unimodal maps with the invariant density given by the symmetric beta distribution. However the solution presented in [7] is a partial and very specialized one. Depending on the chosen symmetry constraints we can get an infinite number of such solutions. In the present paper we go one step further and present the general solution to the IFPP within the class of unimodal maps. A central role is hereby played by the function h_f which parametrizes the space of the solutions to the IFPP. This solution enables us to explore in depth the connection between the dynamics and statistics in one-dimensional systems. Our investigations concentrate on the wide family of the beta distributions. The IFPP is solved for the asymmetric case when the two exponents in the expression for the density are unequal. From the general solution we obtain two special solutions using two different forms for the function h_f . We then calculate the time-correlation functions and the power spectra of the corresponding dynamical systems. The question of the dependence of the statistical characteristics (singularities of the density, long time behaviour of the autocorrelation function) of these systems on their dynamical characteristics (critical points) is addressed. Next we compare for a given density the dependence of the statistical properties on the form of the function h_f . A large variety of the statistical and dynamical behaviour is obtained. Some theoretical predictions concerning the asymptotic decay of the correlations or the value of the Lyapunov exponents [14–17] in fully chaotic dynamical systems can be tested within the class of our examples.

The paper is organized as follows: In section II we present the general solution to the IFPP within the class of unimodal maps. In section III we derive from the general solution of section II a wide family of unimodal maps having as invariant density the beta distribution. This family of maps corresponds to two special solutions of the IFPP: the symmetric betamap (SB) and the special asymmetric betamap (SAB). In section IV we discuss the main characteristics of the maps belonging to the beta family and we study the rich dynamical behaviour which they provide. In section V we calculate the autocorrelation function, the power spectrum and the Liapunov exponent for representative members of the beta family. A connection between the dynamics and the asymptotic decay of correlations is established. Some theoretical models explaining this behaviour are tested. Finally section VI contains

the conclusions and gives a brief outlook with respect to the inclusion of the correlation behaviour into the inverse Frobenius-Perron problem.

II. GENERAL SOLUTION OF THE IFPP FOR UNIMODAL ERGODIC AND CHAOTIC MAPS

Let us consider the variety of dynamical systems which belong to an arbitrary but fixed invariant density. The solution to this inverse problem is of great interest for the numerical simulation of real physical systems as well as the understanding of the relationship between the functional form of the map and the statistical features of its resulting dynamics. In the present section we establish a general representation of all ergodic and chaotic unimodal maps with a given invariant density. This corresponds to the general representation of the solution of the so called inverse Frobenius-Perron problem (IFPP) [8–13] within this class of maps. The starting-equation for the construction of the map is the Frobenius-Perron equation:

$$\rho(y)|dy| = \sum_{x_i=f^{-1}(y)} \rho(x_i)|dx_i| \quad (1)$$

where the summation runs over all preimages of y (for unimodal maps $i = L(left), R(right)$). For any given unimodal $f(x)$ the right or left preimage of y is determined, once the corresponding other one is given. The essential feature of our approach is the inversion of this expression: A prescribed relation between the two preimages reduces the number of independent differentials on the rhs of eq.(1) and allows a following integration. Such a relation may be described by a function $h_f(x)$, mapping the left preimage onto the right one:

$$\begin{aligned} h_f : [0, x_{\max}] &\longrightarrow [x_{\max}, 1] \\ x_R = h_f(x_L) \quad \text{with} \quad f(x_L) &= f(x_R) \end{aligned} \quad (2)$$

where x_{\max} is the position of the maximum of the unimodal map. $h_f(x)$ is a function monotonously decreasing on the defining interval and it is differentiable with the exception of a finite number of points. It obeys the equations:

$$\begin{aligned} h'_f(x) < 0 \quad x \in [0, x_{\max}] \\ h_f(0) = 1 \quad h_f(x_{\max}) = x_{\max} \end{aligned} \quad (3)$$

Substituting h_f in eq.(1) yields:

$$\rho(y)dy = \rho(x_L)dx_L - \rho(h_f(x_L))h'_f(x_L)dx_L \quad (4)$$

Using the definition $\mu(x) = \int_0^x \rho(t) dt$ for the invariant measure eq.(4) can be integrated in $0 < x < x_{\max}$ providing us with the left part $f_L(x) = f(x)|_{[0, x_{\max}]}$ of the map $f(x)$:

$$f_L(x) = \mu^{-1}[\mu(x) - \mu(h_f(x)) + 1] \quad (5)$$

with $\mu(x)$ being invertible and normalized, i.e. $\mu(1) = 1$. The right part of the map, $f_R(x) = f(x)|_{[x_{\max}, 1]}$, is obtained by substitution of $x \rightarrow h_f^{-1}(x)$ in eq.(5). It follows that the map $f(x)$ parametrised through the function $h_f(x)$ and characterised by the invariant measure $\mu(x)$, is given by:

$$f(x) = \begin{cases} \mu^{-1}[\mu(x) - \mu(h_f(x)) + 1] & ; \quad 0 \leq x < x_{\max} \\ \mu^{-1}[\mu(h_f^{-1}(x)) - \mu(x) + 1] & ; \quad x_{\max} \leq x \leq 1 \end{cases} = 1 - |\mu(x) - \mu(H_f(x))| \quad (6)$$

where $H_f(x)$ is given by:

$$H_f(x) = \begin{cases} h_f(x) & ; \quad 0 \leq x < x_{\max} \\ h_f^{-1}(x) & ; \quad x_{\max} \leq x \leq 1 \end{cases} \quad (7)$$

With the above eq.(6) we have found an interesting representation and answer to the IFPP which is the central topic of this paper: All unimodal maps with prescribed invariant measure are given by (6), $h_f(x)$ taking on all possible functional forms obeying (2) and (3). This shows that a fixed invariant measure is a relatively weak constraint to a solution of the inverse problem and there is still a considerable freedom to model the mapping.

Before we apply our method to analyse specific examples we mention an interesting connection between this approach and the approach via conjugation transformations which can also be applied to construct a map with an arbitrary

given (in general nonsymmetric) invariant density. To our knowledge the conjugation transformation method has been applied in the literature only to the restricted case of the construction of a symmetric map with prescribed invariant density [15,16]. We will show below how this approach can be extended to include all unimodal maps. First we recall the basic features of the conjugation transformation approach. More details can be found in the literature [18,19]. Using as a basis the tent map given by: $t(x) = 1 - |2x - 1|$ and applying the conjugation transformation $g(x) = u^{-1} \circ t \circ u(x)$ with $u(0) = 0$, $u(1) = 1$, $u'(x) > 0$ for all $x \in [0, 1]$ and with the additional property $u(x) = 1 - u(1 - x)$ (antisymmetric with respect $x_{max} = \frac{1}{2}$) we can span the space of all doubly symmetric maps (symmetric maps and symmetric invariant densities). The invariant density of the transformed map $g(x)$ is then: $\rho_g(x) = \left| \frac{du(x)}{dx} \right|$. To arrive in an analogous way at a nonsymmetric density while the map remains symmetric we have to use a generalized conjugation transformation:

$$f(x) = U^{-1} \circ t \circ u(x) \quad ; \quad U(x) = u(x) + v(x) \quad (8)$$

For symmetric $f(x)$ the function $v(x)$ must also be symmetric: $v(x) = v(1 - x)$. The two constraints, i.e. that the invariant density of the resulting map $f(x)$ is a prescribed function $\rho(x)$ and that $f(x)$ is symmetric, determine uniquely the transformation functions: $u(x), v(x)$. Defining the symmetric $\mu_+(x) = \frac{1}{2} \int_0^x (\rho(t) - \rho(1 - t)) dt$ and antisymmetric parts $\mu_-(x) = \frac{1}{2} \int_0^x (\rho(t) + \rho(1 - t)) dt$ (with $\mu(x) = \mu_+(x) + \mu_-(x)$) of the invariant measure $\mu(x)$ we find: $u(x) = \mu_-(x)$; $v(x) = \mu_+(x)$. Using the fact that: $\mu_-(x) = \frac{1}{2}(\mu(x) + 1 - \mu(1 - x))$ we get the following expression for the desired map $f(x)$:

$$f(x) = \mu^{-1} [1 - |\mu(x) - \mu(1 - x)|] \quad (9)$$

Comparing equations (6) and (9) we see that they are compatible provided that $h_f(x) = 1 - x$, which corresponds to the correct choice of h_f in (6) for a symmetric solution $f(x)$.

We can now extend the conjugation transformation approach in order to determine also nonsymmetric maps with a given invariant density. For the derivation of eq.(9) we have used a decomposition of the invariant measure in a symmetric and an antisymmetric part (with respect to x_{max}). This decomposition leads us to a symmetric solution. A general decomposition $\mu_+(x), \mu_-(x)$ obeying $\mu_+(x) + \mu_-(x) = \mu(x)$ is given in the following. In the case of unimodal maps we introduce the following components of the measure $\mu(x)$:

$$\begin{aligned} \mu_+(x) &= \frac{1}{2} \int_0^x (\rho(t) + H'_f(t)\rho(H_f(t))) dt \\ \mu_-(x) &= \frac{1}{2} \int_0^x (\rho(t) - H'_f(t)\rho(H_f(t))) dt \end{aligned} \quad (10)$$

with $H_f(x)$ given in eq.(7). Using the generalized conjugation transformation of eq.(8) with $u(x) = \mu_-(x)$ and $v(x) = \mu_+(x)$ we get the solution of eq.(6) to the IFPP. Thus conjugation transformations of the form of eq.(8) with $u(x), v(x)$ chosen as in eq.(10) span the entire space of unimodal maps with a given invariant density $\rho(x)$.

III. AN EXTENSIVE CLASS OF MAPS WITH THE BETA-DISTRIBUTION AS INVARIANT DENSITY

The method to construct an one-dimensional unimodal map with a prescribed invariant density, as proposed in the previous section, applies for all possible forms of the invariant measure $\mu(x)$ and the invariant density $\rho(x)$, respectively. Nevertheless we want to consider a special class of particularly relevant invariant densities $\rho(x)$, namely the two-parametric Beta-distribution:

$$\rho(x) = \frac{x^\alpha (1-x)^\beta}{B(\alpha+1, \beta+1)} \quad \alpha, \beta > -1 \quad (11)$$

These densities are important due to their widespread occurrence and applicability (for example in turbulent reacting flows, diffusion in disordered media, image classification see refs. [20]) as well as their simple form. The special case of a symmetric density ($\alpha = \beta$) with a symmetric solution, i.e. a map obeying ($f(x) = f(1 - x)$), which is unique,

has been already discussed in the literature [7]. We call this solution the doubly symmetric Beta-map (DSB). In the present paper we discuss the general case of an asymmetric invariant density ($\alpha \neq \beta$).

We focus on two solutions of the IFPP with this general asymmetric invariant density, both of which are identical to the DSB in the case $\alpha = \beta$:

- The first solution is symmetric ($f(x) = f(1 - x)$). We call it the symmetric Beta-map (SB).
- The second solution obeys the following constraint:

$$f(x_L) = f(x_R) \quad \text{for } x_L, x_R \text{ with } \rho(x_L) = \rho(x_R), \quad (12)$$

which is only possible if $\alpha \cdot \beta > 0$. We call this solution the Special Asymmetric Beta-map (SAB). In Fig.1 we show an example of such a map for the case $\alpha = -0.9, \beta = -0.6$. The corresponding invariant density is also presented and the notation regarding the imposed constraint of eq.(12) is explained.

In the following we consider only examples where both α and β possess the same sign, i.e. the above criterion is fulfilled. These two types of solutions correspond of course to two different choices for the form of the function $h_f(x)$. For the case of the SB we have $h_f(x) = 1 - x$. The second case is more delicate. It corresponds to an implicitly defined $h_f(x)$. From the condition in eq.(12) and eq.(11) we find:

$$(1 - x_R)x_R^\gamma = (1 - x_L)x_L^\gamma \quad (13)$$

where $\gamma = \frac{\alpha}{\beta}$. Eq.(13) defines h_f and can be solved parametrically. Using $\lambda = \frac{x_L}{x_R}$ we get:

$$x_L = \lambda \frac{1 - \lambda^\gamma}{1 - \lambda^{\gamma+1}} \quad ; \quad x_R = \frac{1 - \lambda^\gamma}{1 - \lambda^{\gamma+1}} \quad (14)$$

with $0 \leq \lambda \leq 1$. Let us now apply the theoretical considerations of section II to derive the expressions for the two types of Beta-maps referred above. The invariant measure corresponding to the density (11) is:

$$\mu_B(x) = \frac{\int_0^x dt t^\alpha (1-t)^\beta}{B(\alpha+1, \beta+1)} = \frac{B(\alpha+1, \beta+1, x)}{B(\alpha+1, \beta+1)} \quad (15)$$

where $B(a, b, z)$ is the incomplete beta function [21]. Using eq.(5) we can determine implicitly the left branch of the solution of the IFPP:

$$B(\alpha+1, \beta+1, f_L(x)) = B(\alpha+1, \beta+1, x) - B(\alpha+1, \beta+1, h_f(x)) + B(\alpha+1, \beta+1) \quad (16)$$

and a similar expression results also for $f_R(x)$:

$$B(\alpha+1, \beta+1, f_R(x)) = B(\alpha+1, \beta+1, h_f^{-1}(x)) - B(\alpha+1, \beta+1, x) + B(\alpha+1, \beta+1) \quad (17)$$

To get the two special solutions referred above we have to substitute in eqs.(16,17) the suitable h_f . As we already mentioned for the SB we choose $h_f(x) = h_f^{-1}(x) = 1 - x$. Taking into account this special form of h_f and the fact that the eqs.(16,17) are valid for $x < x_{max}$ and $x > x_{max}$, respectively (for SB $x_{max} = \frac{1}{2}$), we can recast eqs.(16, 17) into a single equation:

$$B(\alpha+1, \beta+1, y_{SB}) = B(\alpha+1, \beta+1) - |B(\alpha+1, \beta+1, x) + B(\beta+1, \alpha+1, x) - B(\alpha+1, \beta+1)| \quad x \in [0, 1] \quad (18)$$

with $y_{SB} = f_{L,SB}(x)$ for $0 \leq x \leq x_{max}$ and $y_{SB} = f_{R,SB}(x)$ for $x_{max} < x \leq 1$. To calculate the value of the SB for a given x we have to solve eq.(18) numerically using a standard root finding routine. It turns out that the bisection method [22] is well suited for a fast and accurate determination of y_{SB} . In Fig.2a we present 4 characteristic members of the class of symmetric beta-maps calculated numerically using (18).

Let us now return to the SAB case. The calculation of the map y_{SAB} is a little more tedious. For a given x we use eq.(13) to find numerically x_R (x_L) if $x < x_{max}$ (if $x > x_{max}$). Note that for the SAB $x_{max} = \frac{\alpha}{\alpha+\beta}$. The numerical solution to eq.(13) can be easily obtained using the bisection method. Then we apply eq.(6) to determine y_{SAB} :

$$B(\alpha+1, \beta+1, y_{SAB}) = \begin{cases} B(\alpha+1, \beta+1, x) - B(\alpha+1, \beta+1, x_R) + B(\alpha+1, \beta+1) & ; \quad 0 \leq x < x_{max} \\ B(\alpha+1, \beta+1, x_L) - B(\alpha+1, \beta+1, x) + B(\alpha+1, \beta+1) & ; \quad x_{max} \leq x \leq 1 \end{cases} \quad (19)$$

Again we have to find the root y_{SAB} of eq.(19) numerically using the bisection method. We emphasize that the bisection procedure in solving eq.(19) could be circumvented in the case that the inverse of the incomplete beta function $B^{-1}(a, b, z)$ is given explicitly. The calculated SAB maps, for the same choice of the values of α and β as in Fig.2a, are presented in Fig.2b.

For both types of maps SB and SAB a dynamical route to the fully chaotic and ergodic state can be constructed applying the method described in [7]. Using the numerical solutions to eqs.(18,19) we calculated trajectories for the corresponding maps for different values of the parameters α and β . Averaging over a long trajectory of each map we reproduced with a good agreement the invariant densities given as the input for the construction of these maps. We mention that, due to computational accuracy reasons, for α, β values close to -1 it is necessary to calculate $1 - y$ instead of y in that range of x for which $y(x) \approx 1$.

Finally let us introduce the concept of the complementary beta-map, CB. Two maps $y(x)$ and $\tilde{y}(x)$ belonging to SB or SAB are called complementary, if their invariant densities $\rho(x)$ and $\tilde{\rho}(x)$ are transformed into each other by changing x to $1 - x$. Considering the Frobenius-Perron equation, which is the starting point for the construction of both SB and SAB maps, the following relation can be derived:

$$B[\alpha + 1, \beta + 1, y(x)] = B[\beta + 1, \alpha + 1, \tilde{y}(1 - x)] \quad (20)$$

Complementary maps agree with respect to certain dynamical features, e.g. the Lyapunov-exponent, as shown below.

IV. ANALYTICAL AND DYNAMICAL PROPERTIES OF THE SB AND SAB

Many features of the dynamics generated by a discrete map do not depend on the dynamical law as a whole, but only on its local behaviour in certain regions of the phase space. In particular for the case of unimodal maps the order of the maximum turns out to be responsible for some interesting quantities characterising the underlying dynamics like the singularities of the invariant density at $x = 0$ and $x = 1$, the decay constant of the autocorrelation and the scaling parameter of the Feigenbaum bifurcation route [23]. The order ν_m of a map at its maximum x_{\max} , is defined as the exponent in the approximation:

$$f(x) \approx 1 - (x - x_{\max})^{\nu_m} \quad \text{for} \quad x \approx x_{\max} \quad (21)$$

In an analogous way we can define the order of the map at the end points: $x = 0, 1$. In the following we will determine the corresponding exponents ν_m, ν_0, ν_1 for the SB and SAB.

(a) The SB case

One can easily utilise the Frobenius-Perron-equation

$$\frac{dy}{dx} = \frac{x^\alpha(1-x)^\beta + x^\beta(1-x)^\alpha}{y^\alpha(1-y)^\beta} \quad (22)$$

where $y = f(x)$ is the SB-map. For $x \rightarrow x_{\max} = \frac{1}{2}$ the nominator on the rhs is finite which yields $\frac{dy}{dx} \propto \frac{1}{y^\alpha(1-y)^\beta}$. Assuming $\nu_{m,SB}$ to be the order of the map in the maximum, i.e. $(1-y) \propto (x - \frac{1}{2})^{\nu_{m,SB}}$ one gets

$$\nu_{m,SB} = \frac{1}{\beta + 1} \quad (23)$$

Expanding eq.(18) around the points $x = 0$ and $x = 1$ and taking into account that $y_{SB} \rightarrow 0$ for $x \rightarrow 0$ or $x \rightarrow 1$ we find the exponents $\nu_{0,SB}$ and $\nu_{1,SB}$ to be:

$$\nu_{0,SB} = \nu_{1,SB} = \frac{\min(\alpha, \beta) + 1}{\alpha + 1} \quad (24)$$

(b) The SAB case

Determining the order of the SAB at its maximum $x = \frac{\alpha}{\alpha + \beta}$ turns out to be slightly more complicated compared to the case of the SB due to the implicit form of h_f . The derivative $\frac{dy}{dx}$ of the SAB $y = f(x)$ is given by the Frobenius-Perron equation. In terms of the parametric solution $x_R(\lambda), x_L(\lambda)$ of eq.(14) we get:

$$\frac{dy(x)}{dx} = \begin{cases} \frac{dy(\lambda)}{d\lambda} / \frac{dx_R}{d\lambda} & , \quad 0 < x < x_{max} \\ \frac{dy(\lambda)}{d\lambda} / \frac{dx_L}{d\lambda} & , \quad x_{max} < x < 1 \end{cases} \quad (25)$$

The limit $(x - x_{max}) \rightarrow 0$ corresponds to the limit of the above equation for $\lambda \rightarrow 1$. Higher derivatives $\frac{d^n y}{dx^n}$ are obtained by differentiating $\frac{d^{n-1}y}{dx^{n-1}}$ with respect to λ and subsequent dividing by $\frac{dx_L}{d\lambda}$ or $\frac{dx_R}{d\lambda}$, respectively. The leading behaviour of the left or right derivative $\frac{d^n y}{dx^n}|_{L,R}$ for $y \rightarrow 1$ (which corresponds to $(x - x_{max}) \rightarrow 0$) is given by:

$$\frac{d^n y}{dx^n}|_{L,R} \sim \frac{\frac{d^n y}{d\lambda^n}}{\left(\frac{dx_{L,R}}{d\lambda}\right)^n} \quad (26)$$

A straightforward but tedious calculations shows that $\frac{d^n y}{dx^n} \propto \frac{1}{(1-y)^{n\beta+(n-1)}}$. The exponent of $(1-y)$ vanishes for a value

$$n = \nu_{m,SAB} = \frac{1}{\beta + 1} \quad (27)$$

which gives the order $\nu_{m,SAB}$ of the SAB at the maximum. Expanding eq.(19) around the endpoints $x = 0, 1$ we get:

$$\nu_{0,SAB} = \min(1, \frac{\alpha(1+\beta)}{\beta(1+\alpha)}) \quad ; \quad \nu_{1,SAB} = \min(\frac{\beta}{\alpha}, \frac{1+\beta}{1+\alpha}) \quad (28)$$

According to the behaviour of the SB and the SAB near the characteristic points $0, 1, x_{max}$ we can classify the forms of maps which we obtain for different values of α and β as follows:

- The region $x \approx x_{max}$: The order of the map at x_{max} , given by $\nu_m = \frac{1}{1+\beta}$, is a common quantity for all beta-maps. Maps with $\beta < 0$ are differentiable and therefore flat at x_{max} . With β approaching -1 , the maps become increasingly flatter. $\beta > 0$ results in a cusp-like shape of the map near x_{max} .
- The zero points 0 and 1:

As far as the form of the maps near the points 1 and 0 is concerned, four limiting cases with certain values for α and β can distinguished.

- $\alpha \approx 0, \beta \approx 1$:

The maps belonging to both SAB and SB show divergent derivatives $f'(0) \rightarrow \infty, f'(1) \rightarrow -\infty$. The map itself has a convex shape. As the maximum of the SAB is in $[0, \frac{1}{2}]$, the right branch of the map, containing the unstable fixed point, is more shallow than that of the corresponding SB map.

- $\alpha \approx 1, \beta \approx 0$:

At $x = 0$, both the SB as well as the SAB map develop a slope $f'(0) \rightarrow 1$ which enables them to generate intermittent dynamics. Since the SB are symmetric we have $f'(1) \rightarrow 1$. The derivatives of the SAB maps however show divergent behaviour, $f'(1) \rightarrow -\infty$

The SB and SAB maps are identical to the DSB for $\alpha = \beta$. The derivatives of the maps $f'(0)$ and $f'(1)$ take on finite values.

- $\alpha = \beta \approx 0$: The limit $\alpha = \beta \rightarrow 0$ of the DSB is the tent map $f'(0) \rightarrow 2, f'(1) \rightarrow -2$.

- $\alpha = \beta \approx 1$:

The values of $f'(0) = f'(1)$ are still finite, but increase unbounded in the limit $\alpha = \beta \rightarrow 1$. The map is extremely flat about the maximum and takes on values very close to 1 in nearly the whole interval $[0, 1]$.

The dynamics generated by both the SAB and the SB result in singularities of the invariant density at $x = 0, 1$ for $-1 < \alpha, \beta < 0$. Although the strengths of these singularities can be directly read from eq.(11) it is of interest to explore how they are determined through the order of the map at the maximum and at the endpoints 0, 1. The strength of the singularity at $x = 1$ is determined by the order of the maximum only. As the order of the map for both SB and SAB at its maximum is given by $\nu_m = \frac{1}{\beta+1}$, the expansion of the map in this region reads

$$1 - y \approx |1 - x_{max}|^{\nu_m} = |1 - x_{max}|^{\frac{1}{\beta+1}} \quad (29)$$

Near x_{max} the invariant measure is a smooth function. Using eq.(1) we can therefore write $\rho(y) |dy| \propto |dx|$. The dependence of the differential $|dy|$ on x is given by $|dy| \approx \frac{1}{\beta+1} (x - \frac{1}{2})^{\frac{1}{\beta+1}-1} |dx|$. If we now make the ansatz $\rho(y) \propto (1-y)^{\tilde{\beta}}$ for the invariant density at $x \approx 1$, the Frobenius-Perron equation in orders of x reads

$$(x - x_{max})^{\tilde{\beta} \frac{1}{\beta+1}} (x - x_{max})^{\frac{1}{\beta+1}-1} |dx| \propto |dx| \implies \tilde{\beta} \frac{1}{\beta+1} + \frac{1}{\beta+1} - 1 = 0 \implies \tilde{\beta} = \beta \quad (30)$$

We therefore conclude that the strength of the singularity of the invariant density at $x = 1$ for both types of maps (SB and SAB) is given implicitly by the order of the dynamic law at its maximum.

The determination of the singularity at $x = 0$ is more intricate. We will study in detail the case of the SB maps. The SAB maps can be treated in an analogous way. For the SB family the Frobenius-Perron equation can be written in the form:

$$\rho(y_{SB}) |dy_{SB}| = [\rho(x) + \rho(1-x)] |dx|, \quad (31)$$

Using eq.(24) the SB at $x \approx 0$ is approximately given by $y_{SB} \approx x^{\frac{\min(\alpha, \beta)+1}{\alpha+1}}$. Let us make the ansatz $\rho(y_{SB}) \propto y_{SB}^{\tilde{\alpha}}$ for the singularity of the invariant density at $y_{SB} = 0$. For $x \approx 0$ $\rho(x)$ and $\rho(1-x)$ possess the singularities $\tilde{\alpha}$ and β , respectively. Therefore the Frobenius-Perron equation reads

$$x^{\tilde{\alpha} \frac{\min(\alpha, \beta)+1}{\alpha+1}} x^{\frac{\min(\alpha, \beta)+1}{\alpha+1}-1} |dx| \propto x^{\min(\tilde{\alpha}, \beta)} |dx| \quad (32)$$

$$\implies \tilde{\alpha} \frac{\min(\alpha, \beta)+1}{\alpha+1} + \frac{\min(\alpha, \beta)+1}{\alpha+1} - 1 = \min(\tilde{\alpha}, \beta) \quad (33)$$

Two cases have to be considered:

- The first possibility is $\min(\alpha, \beta) = \beta$. In this case eq.(33) yields $\tilde{\alpha}(\beta+1) + (\beta - \alpha) = (\alpha+1)\min(\tilde{\alpha}, \beta)$ and therefore

$$\min(\tilde{\alpha}, \beta) = \frac{\beta(\tilde{\alpha}+1) + (\tilde{\alpha}-\alpha)}{\alpha+1} \min(\tilde{\alpha}, \beta) \quad (34)$$

with the solution $\alpha = \tilde{\alpha}$. The singularity at $x = 0$ is given by the parameter α as expected.

- The case $\alpha < \beta$ demands slightly more attention. The order of the map in $x = 0$ and $x = 1$ is one, according to eq.(24). This makes the dynamics a candidate for intermittency, which is characterised by an expansion of the map near a marginally unstable fixed point of the form

$$y(x) \approx x + \epsilon x^z \quad x \rightarrow 0 \quad (35)$$

The order of the next-to leading term, z , determines essentially the statistical properties of the dynamical law near $x = 0$. In ref. [14] it was shown, that a symmetric map, with a maximum of order ν_m and of the form (35) at $x = 0$, generates an invariant density, which has a singularity of the order

$$\tilde{\alpha} = \frac{1}{\nu_m} - z \quad (36)$$

at $x = 0$. Using the implicit representation of the SB map:

$$B(\alpha+1, \beta+1, y_{SB}) = B(\alpha+1, \beta+1, x) + B(\beta+1, \alpha+1, x), \quad x < \frac{1}{2} \quad (37)$$

and expanding the incomplete Beta-functions around $x = 0$ with the help of the formula:

$$B(\alpha+1, \beta+1, t) \approx \frac{t^{\alpha+1}}{\alpha+1} - \beta \frac{t^{\alpha+2}}{\alpha+2} \quad (38)$$

we find:

$$\frac{y_{SB}^{\alpha+1}}{\alpha+1} \approx \frac{x^{\alpha+1}}{\alpha+1} + \frac{x^{\beta+1}}{\beta+1} \quad (39)$$

It follows that:

$$y_{SB} \approx x \left(1 + \frac{\alpha+1}{\beta+1} x^{\beta-\alpha} \right)^{\frac{1}{\alpha+1}} \approx x + \frac{1}{\beta+1} x^{\beta-\alpha+1} \quad (40)$$

Therefore the term next to the leading one is of order $z = \beta - \alpha + 1$. Using eq.(36) and $\nu_m = \frac{1}{\beta+1}$ we find $\tilde{\alpha} = \beta + 1 - (\beta - \alpha + 1) = \alpha$, i.e. the correct strength of the singularity at $x = 0$ is reproduced.

At the end of this section let us discuss the different kinds of dynamics which are generated by the different types of maps in the two classes SAB and SB. Depending on the values of α and β , there are two eyecatching types of dynamical behaviour:

- $0 > \alpha > \beta$

The trajectories of both SB and SAB maps are characterised by an oscillatory motion around the unstable fixed point in the right interval of monotony of the map. The orbit leaves the region close to the fixed point, where the linear approximation of the map is valid, exponentially fast. This phase of the dynamics is highly correlated. The time which a corresponding trajectory spends in the neighbourhood of the unstable fixed point is for SAB maps typically larger than for SB maps. The reason for this is the fact that the derivations of the SAB maps are usually in a larger region closer to -1 than those of the SB maps. After leaving this regime we encounter an oscillatory motion of the orbit about the maximum. In this case the left and the right branch of the map are visited alternately. As the parts of the map visited are nearly symmetric with respect to the axis $y(x) = x$, a nearly stable orbit with period two occurs. This peculiar feature of the map is more common for the SB maps. The two singularities of the invariant density are build up by these oscillations. As the centre of the oscillations is shifted to the right of $\frac{1}{2}$, the singularity at $x = 1$ is stronger than the one at $x = 0$.

- $\alpha < \beta < 0$

The dynamics developed by both the SB and the SAB maps is dominated by the intermittent behaviour near the marginally unstable fixed point at $x = 0$. The trajectories show an interplay of chaotic motion and laminar phases in the region of $x = 0$. The comparison of the maps belonging to the two classes shows nicely the detailed balance of the system generating the same invariant density: For a SAB the exponent z in the expansion $y(\epsilon) \approx x + \epsilon^z$, $\epsilon \ll 1$ is much closer to 1 than for the corresponding SB map and the region of the map where this expansion holds is larger. Therefore the orbit tends to be captured for a longer time in this region. However, due to the diverging derivative of the SAB map at $x = 1$, the laminar region is visited less often, which partially cancels the above effect.

V. LYAPUNOV EXPONENTS, AUTOCORRELATIONS AND POWER SPECTRA FOR SB AND SAB

In this section we derive some dynamical and statistical properties of characteristic members of the SB and SAB classes of maps. First we consider the Lyapunov-exponents which are a measure for the degree of chaoticity. As the derivatives of both classes SB and SAB are obtained from the Frobenius-Perron equation, the Lyapunov-exponents $\Lambda_{\alpha,\beta}^{SB}$ and $\Lambda_{\alpha,\beta}^{SAB}$, respectively can be calculated using the definition $\Lambda = \int_0^1 \rho(x) \ln \left| \frac{dy(x)}{dx} \right| dx$. The implicit form of $y(x)$ prevents an analytical treatment. Therefore we have calculated $\Lambda_{\alpha,\beta}^{SB}$ and $\Lambda_{\alpha,\beta}^{SAB}$ numerically for different values of $-1 < \alpha, \beta < 0$, using the equations (18) and (19), respectively. Both Lyapunov-exponents show similar features as functions of α and β . Most striking is the symmetry

$$\Lambda_{\alpha,\beta}^{SB} = \Lambda_{\beta,\alpha}^{SB} \quad \Lambda_{\alpha,\beta}^{SAB} = \Lambda_{\beta,\alpha}^{SAB} \quad (41)$$

i.e. the Lyapunov-exponent stays the same when switching from Beta-maps to the complementary ones, given in eq.(20). This symmetry is even more astonishing, since it connects two very different kinds of dynamics with the same Lyapunov-exponent, i.e. with the same degree of chaoticity. The value of the Lyapunov exponent is maximal ($\ln 2$) for the doubly symmetric case $\alpha = \beta$ and decreases as $|\alpha - \beta|$ increases. This can be at best seen in Fig.3 where we show the Lyapunov exponent $\Lambda_{\alpha,\beta}^{SAB}$ as a function of the parameters α, β . The decrease in the degree of chaoticity for

the case $\alpha < \beta$ is caused by the frequent occurrence of almost regular intermittent intervals while in the case $\alpha > \beta$ it is caused by the dominating hopping of the orbit around the unstable fixed point of the map.

Let us now turn to the calculation of the autocorrelation function $C(n)$ for the SB and SAB members. Again two types of maps in the SB and SAB classes have to be distinguished:

- $\alpha > \beta$

The correlation function is oscillating with period 2 and decays exponentially fast. This is a consequence of the oscillatory motion of the orbit about the unstable fixed point. The decay of the envelope is slower for maps with $|\beta - \alpha|$ large, since the corresponding map has a more shallow slope of the right interval of monotony, which allows long lasting oscillations. The mean decay time of the SB maps (see Fig.4a) is much shorter compared to those of the SAB maps (see Fig.4b). This is caused by the fact that the symmetry of the map restricts the length of the highly correlated, oscillating phases of the orbit.

- $\alpha < \beta$

The intermittent dynamics results in a correlation function, which decays algebraically in the long time regime according to $C(n) \propto n^{-\eta}$. For weak intermittent dynamics the decay exponent η can be estimated analytically. For this aim we use the map:

$$y(\epsilon) = \epsilon + a \epsilon^z + \dots \quad 0 < \epsilon \ll 1 \quad (42)$$

Assuming that the invariant density $\rho(x)$ near the centre of intermittency is given by $\rho(\epsilon) \propto \epsilon^\alpha \quad 0 < \epsilon \ll 1, -1 < \alpha, 1 < z$ and following [14] we derive the following scaling relation describing the autocorrelation function in the limit of distinctive intermittent behaviour, i.e. $0 < z - 1 \ll 1$ and for $n \rightarrow \infty$:

$$C(n) \approx K \left(1 + \frac{n}{n_0} \right)^{-\eta} \quad (43)$$

with

$$\eta = \frac{1 + \alpha}{z - 1} \quad > 0 \quad \text{and} \quad \frac{1}{n_0} = (z - 1) a (\bar{x} + 1)^{z-1} \quad (44)$$

where K is a constant characteristic for the system. This behaviour takes account of the long and highly correlated laminar sections of the orbit. The characteristic exponent η decreases with increasing $|\beta - \alpha|$ and thus corresponds to a slower decay of the correlation. For shorter times a transient behaviour leading into the algebraic decay can be seen. The correlation of systems generated by SB maps (Fig.5a) decay faster compared to those SAB maps with the same values for α and β (Fig.5b). The knowledge of the order of the SB maps in the maximum point and the zeros at $x = 0$ and $x = 1$ allows a comparison of the characteristic exponent η_{numer} obtained numerically with the value η_{approx} obtained by the continuous time approximation in [14]. It shows a fair agreement that becomes better for maps which possess a more pronounced intermittency. In this case the values of α and β differ most.

α	β	z	η_{approx}	η_{numer}
-0.8	-0.6	1.2	1.0	1.09
-0.6	-0.4	1.2	2.0	1.86
-0.6	-0.2	1.4	1.0	0.81
-0.8	-0.2	1.6	0.33	0.33

TABLE I. Decay constants η_{approx} and η_{numer}

The corresponding power spectrum of both the SB and SAB maps, defined by

$$S(f) = \frac{1}{\sqrt{2\pi}} \int_{-\infty}^{\infty} C(\tau) e^{-2\pi i f \tau} d\tau \quad (45)$$

shows the typical power-law scaling behaviour:

$$S(f) \propto f^{-\eta} \quad (46)$$

for low frequencies. For higher frequencies $S(f)$ differs from this rule since it reflects the transient regime of the correlation function. This behaviour of the power spectrum in the intermittent regime is illustrated in Fig.6a,b for different sets of α, β .

VI. CONCLUSIONS

We have presented a general solution to the inverse Frobenius-Perron problem for the case of unimodal one-dimensional maps. This solution allows us to cover the entire space of fully chaotic unimodal maps with given invariant density. It is shown that the general solution can also be obtained by a suitably defined conjugation transformation. Using this general representation one can find infinitely many particular solutions. To illustrate our method we applied it to obtain two classes of dynamical systems possessing the two parametric beta-probability function as the invariant density. We calculated the Lyapunov exponents, autocorrelation functions and power spectra for these maps and studied the properties of the obtained solutions in a twofold manner: First we observed for given values of the parameters of the invariant density the changes in the dynamical and statistical properties for systems corresponding to different partial solutions of the Frobenius-Perron equation. We then varied the parameters of the invariant density remaining within a certain class of partial solutions. From our studies we conclude that two typical properties dominate the dynamics for unimodal beta maps. The first property is the hopping of the chaotic trajectory around the unstable fixed point of the map which leads to an exponential decay of correlations. The decay constant depends on the explicit form of the special solution for given parameters of the invariant density. The second possibility is the intermittent scenario: the chaotic trajectory possesses extended laminar phases in the neighbourhood of $x = 0$. The correlations in this case decay with a power-law. Theoretical investigations predict that the characteristic exponent in this power-law decay is determined through the singularities of the invariant density at the center of intermittency ($x = 0$) as well as the derivative of the map at this point. We tested these estimations and found a satisfactory agreement with our numerical calculations.

Thus our approach to the inverse Frobenius-Perron problem allows us to determine one-dimensional maps with a rich variety of dynamical behaviour and enables us to perform accurate calculations for physical observables even in the case where the ergodic limit is computationally inaccessible (intermittency). The obtained general solution involves the function h_f and one might therefore use this degree of freedom to design dynamical laws with more prescribed quantities than the invariant density. One step in this direction would be to solve the inverse Frobenius-Perron problem with the additional constraint of a given autocorrelation function. Using the parametrisation (6) of the general solution to the Frobenius-Perron equation it should be in principle possible to design a map which is closest to a certain given correlation behaviour. A detailed investigation of this problem is in progress [24].

[1] M.J. Feigenbaum, J. Stat. Phys. **19**, 25 (1978); **21**, 669 (1979).
[2] J.P. Crutchfield, J.D. Farmer and B.A. Huberman, Phys. Rep. **92**, 45 (1982).
[3] P. Manneville and Y. Pomeau, Phys. Lett. **75A**, 1 (1979); Physica D **10**, 219 (1980).
[4] T. Geisel, J. Nierwetberg, Phys. Rev. Lett. **48**, 7 (1982); Phys. Rev. A **29**, 2305 (1984).
[5] J.E. Hirsch, B.A. Huberman and D.J. Scalapino, Phys. Rev. A **25**, 519 (1981).
[6] T. Geisel, A. Zacherl and G. Radons, Phys. Rev. Lett. **59**, 2503 (1987).
[7] F.K. Diakonos and P. Schmelcher, Phys. Lett. **211A**, 199 (1996).
[8] A. Baranovsky and D. Daems, Int. J. Bif. and Chaos **5**, 1585 (1995).
[9] S. Koga, Progr. of Theor. Phys. **86**, 991 (1991).
[10] D. Ghikas, Lett. in Math. Phys. **7**, 91 (1983).

- [11] C.C. Grosjean, J. Math. Phys. **28**, 1265 (1987).
- [12] G. Paladin and S. Vaienti, J. Math. Phys. **A21**, 4609 (1988).
- [13] F.Y. Hunt and W.M. Miller, J. Stat. Phys. **66**, 535 (1992).
- [14] S. Grossmann and H. Horner, Z. Phys. B **60**, 79 (1985).
- [15] S. Grossmann and S. Thomae, Z. Naturforsch. **32 a**, 1353 (1977).
- [16] H. Mori, B. So and T. Ose, Progr. of Theor. Phys. **66**, 1266 (1981).
- [17] H. G. Schuster, *Deterministic Chaos*, VCH, Weinheim (1995).
- [18] G. Gyorgyi and P. Szepfalusy, Z. Phys. B **55**, 179 (1983).
- [19] A. Csordas, G. Gyorgyi, P. Szepfalusy and T. Tel, Chaos **3**, 31 (1993).
- [20] C.P. Lowe, P. Frenkel and M.A. van der Foef, J. Stat. Phys. **87**, 1229 (1997); S.S. Girimaji, Phys. of Fluids A **4**, 2875 (1992); ibid. 2529; R.L. Gaffney Jr., J.A. White, S.S. Girimaji and J.P. Drummond, Comp. Sys. in Eng. **5**, 117 (1994); E.R. Weeks, J.S. Urbach and H.L. Swinney, Physica D **97**, 291 (1996); K. Arai, Y. Terayama and T. Arata, IGARSS '95, IEEE **2**, 1263 (1995).
- [21] I.S. Gradshteyn and I.M. Ryzhik, *Tables of Series, Products and Integrals*, Academic Press (1994).
- [22] W.H. Press, B.P. Flannery, S.A. Teukolsky and W.T. Vetterling, *Numerical Recipes*, Cambridge University Press, Cambridge (1992).
- [23] E. Ott, *Chaos in Dynamical Systems*, Cambridge University Press, Cambridge (1993).
- [24] F.K. Diakonos and P. Schmelcher, in preparation.

FIGURE CAPTIONS

FIG. 1. The SAB map for $\alpha = -0.9, \beta = -0.6$ and the corresponding invariant density.

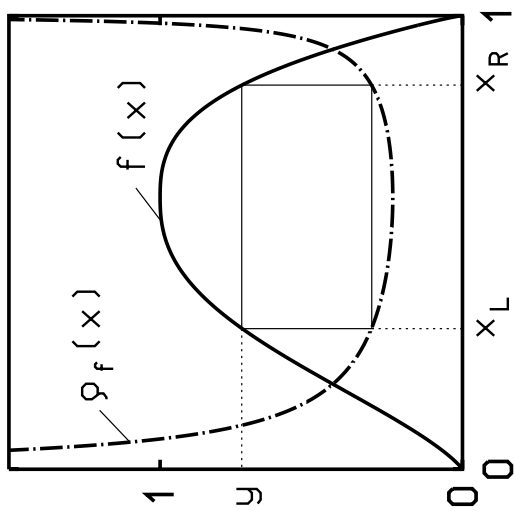
FIG. 2. Characteristic members of the family of maps with the beta-distribution as invariant density: (a) 4 Maps belonging to the SB class. (b) The corresponding 4 maps of the SAB class.

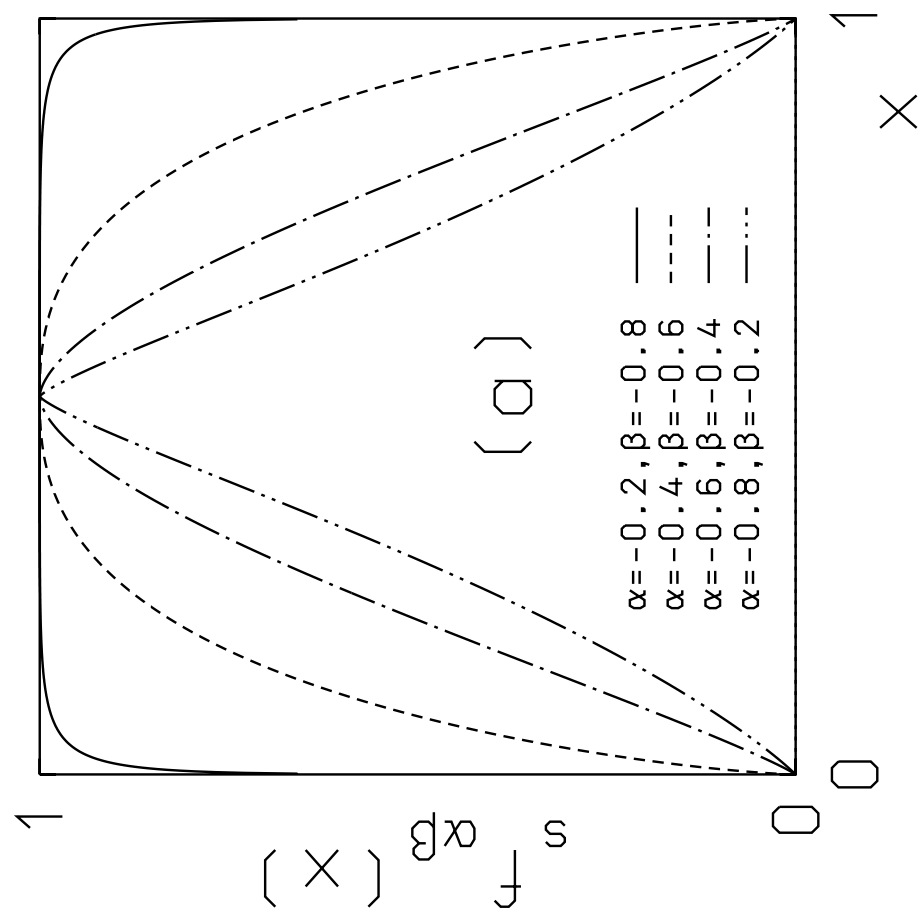
FIG. 3. The Lyapunov exponent $\Lambda_{\alpha,\beta}$ for the SAB class as a function of α, β .

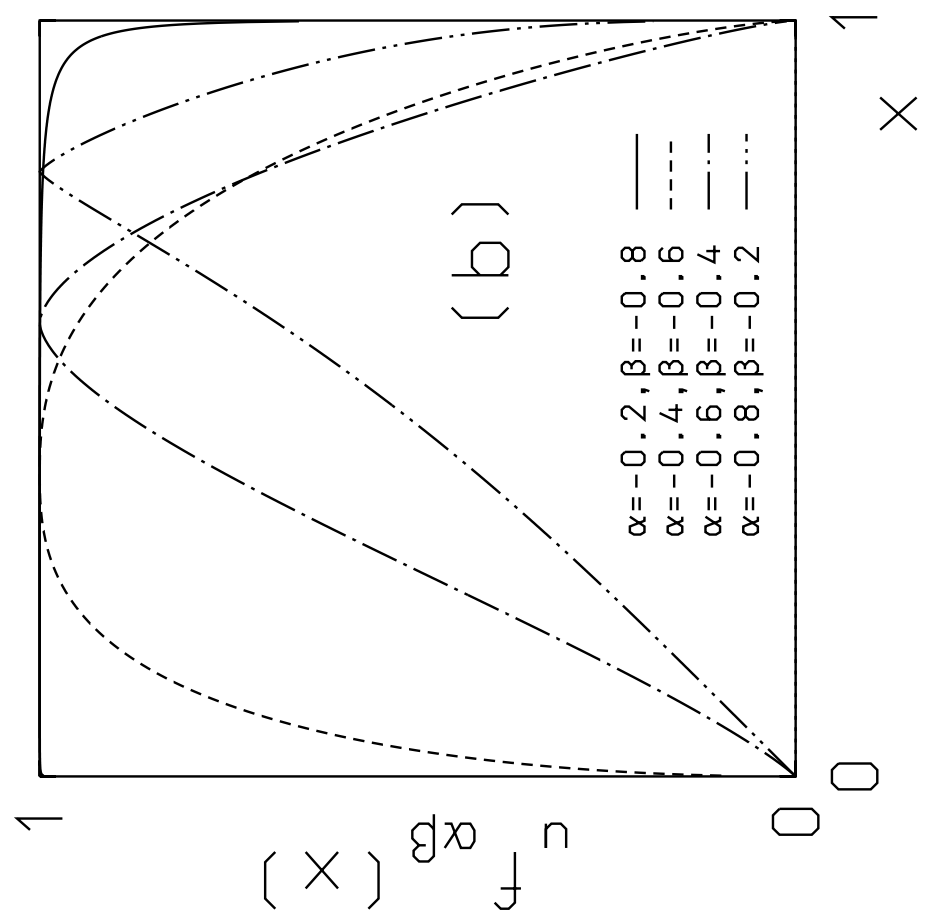
FIG. 4. The absolute value of the autocorrelation function $|C_{\alpha,\beta}|$ for different values of α, β and in the regime $\alpha > \beta$ (exponential regime): (a) for SB maps. (b) for maps belonging to the SAB class.

FIG. 5. The absolute value of the autocorrelation function $|C_{\alpha,\beta}|$ for different values of α, β and for $\alpha < \beta$ (intermittent regime): (a) for SB maps. (b) for maps belonging to the SAB class.

FIG. 6. The square of the absolute value of the power spectrum $S(f)$ as a function of the frequency f for different values of α, β and for $\alpha < \beta$ (intermittent regime): (a) for SB maps. (b) for maps belonging to the SAB class.







$\wedge_{\alpha, \beta}$ 